

# The exponential Lagrangian mean

Abhijeet Minz<sup>1</sup>†, Lois E. Baker<sup>1</sup>, Hossein A. Kafiabad<sup>2</sup> and Jacques Vanneste<sup>1</sup>

<sup>1</sup>School of Mathematics and Maxwell Institute for Mathematical Sciences, University of Edinburgh, Edinburgh EH9 3FD, UK

<sup>2</sup>Department of Mathematical Sciences, Durham University, Durham DH1 3LE, UK

Lagrangian averaging is a valuable tool for the analysis and modelling of multiscale processes in fluid dynamics. The numerical computation of Lagrangian averages from simulation data is considered challenging, however. In response, we develop a straightforward form of Lagrangian (time) averaging – exponential averaging – and derive simple partial differential equations that govern the evolution of the Lagrangian mean fields. These equations can be solved at minimum cost as part of the numerical simulation of fluid models, using the same time and space discretisation as for the dynamical equations.

We implement exponential averaging in the rotating shallow-water model and demonstrate its effectiveness at filtering out large-amplitude Poincaré waves while retaining the salient features of an underlying turbulent flow. We generalise the computation of exponential Lagrangian means from scalar to tensor fields and apply the generalisation to the computation of the Lagrangian mean momentum and of the related pseudomomentum.

## 1. Introduction

Many fluid dynamical phenomena involve temporal and spatial scales that cannot be fully resolved by measuring instruments or numerical simulations. Their modelling requires coarse graining, typically in the form of temporal or spatial averaging of the equations of motion, and the parameterisation of the impact of the unresolved scales. To this end, Lagrangian averaging, whereby averages are computed along fluid trajectories, has advantages over the more straightforward Eulerian averaging. These advantages stem from the preservation under Lagrangian averaging of the advective structure of the equations of motion, leading to valuable properties including the conservation of Lagrangian mean vorticity and circulation in the absence of dissipation and forcing.

A conceptual framework for Lagrangian averaging is provided by the generalised Lagrangian mean (GLM) theory of Andrews & McIntyre (1978) (see Bühler 2014, for a comprehensive introduction). Its practical use, with temporal averaging substituted for the abstract averaging of GLM, has however been hampered by the challenges posed by the numerical computation of Lagrangian means from simulation data. Most implementations to date (Nagai *et al.* 2015; Shakespeare & Hogg 2017, 2018, 2019; Shakespeare *et al.* 2021; Bachman *et al.* 2020; Jones *et al.* 2023) rely on tracking a large number of particles. This is computationally costly and often does not deliver Lagrangian mean fields in full agreement with the GLM definitions. Recent papers by Kafiabad (2022) and Kafiabad & Vanneste (2023, hereafter KV23) develop an approach based on the formulation of partial differential equations (PDEs) satisfied by the Lagrangian mean fields. These PDEs can be solved on the fly, together with the dynamical equations and using the same spatial discretisation. These papers employ a straightforward ‘top-hat’ time averaging but the approach generalises to more sophisticated frequency filters (Baker *et al.* 2024).

† Email address for correspondence: Abhijeet.Minz@ed.ac.uk

This approach remains costly in that independent evolutionary PDEs are integrated over (fast) time to derive the mean field at a single (slow) time. The process then needs to be repeated for each slow time at which averaged fields are desired. There is, however, one particular definition of the time mean that avoids this complication. This is the exponential mean, obtained by convolving the signal with a truncated exponential, which enjoys the unique property of satisfying a closed (first order) differential equation (§2). Its benefit for Lagrangian averaging were pointed out to the authors by O. Bühler.

The first aim of this paper is to adapt the approach of KV23 to the exponential mean. This leads to PDEs for the Lagrangian mean fields that share a single time variable with the dynamical equations and can therefore be solved in tandem with them, with little overheads. We derive these PDEs for the Lagrangian averaging of scalar fields (§3). We then demonstrate their value with an application to a rotating shallow-water flow that combines a slowly evolving turbulent flow with a large-amplitude fast Poincaré wave (§4).

The second aim of this paper is to extend the computation of Lagrangian means, in particular of the exponential mean, to tensor fields. This is motivated by the need to average the dynamical variables of the fluid dynamical equations which are typically not just scalars. This is vital if GLM theory is to be used as a practical modelling tool. We formulate the averaging of tensors and apply it to two fields extracted from the shallow-water flow simulation: momentum and mass, interpreted as 1- and 2-forms, respectively (§5). This interpretation is rooted in the geometric view of GLM developed by Gilbert & Vanneste (2018) (see also Holm 2002*a,b*; Gilbert & Vanneste 2024). We also compute the pseudomomentum and the mean flow Jacobian, important dynamical fields that naturally emerge in this view (Andrews & McIntyre 1978; Bühler & McIntyre 1998; Bühler 2014).

Overall, this paper demonstrates the effectiveness and simplicity of implementation of the exponential mean which could make it the go-to method for the computation of Lagrangian means.

## 2. Lagrangian and exponential means

The GLM time average is defined as follows. Given the flow map  $\varphi$ , such that  $\varphi(\mathbf{a}, t)$  is the position at time  $t$  of a fluid particle labelled by  $\mathbf{a}$ , we first define a mean flow map by

$$\bar{\bar{\varphi}}^i(\mathbf{a}, t) = \overline{\varphi^i(\mathbf{a}, \cdot)}(t), \quad (2.1)$$

where the superscript  $i$  indicates the coordinate and the overbar on the right-hand side denotes any moving time average evaluated at time  $t$ . We emphasise that this construction depends on choosing a coordinate representation of the flow map, since the average of the flow map itself (as opposed to its coordinate representation) is ill defined. We use the unconventional double-bar notation of Gilbert & Vanneste (2024) as a reminder of this. The Lagrangian mean of scalar field  $g(\mathbf{x}, t)$  is defined by

$$\bar{g}^L(\bar{\bar{\varphi}}(\mathbf{a}, t), t) = \overline{g(\varphi(\mathbf{a}, \cdot), \cdot)}(t). \quad (2.2)$$

In words, the Lagrangian mean  $\bar{g}^L(\mathbf{x}, t)$  is the time average of  $g$  following the trajectory of the particle whose mean position at  $t$  is  $\mathbf{x} = \bar{\bar{\varphi}}(\mathbf{a}, t)$ .

KV23 develop an approach for the computation of Lagrangian means of the form (2.2) based on the solution of PDEs. They implement their approach for the ‘top-hat’ mean, that is, straightforward unweighted integration over a time interval  $T$ . This is extended by Baker *et al.* (2024) to the case of a general weighted mean. In this paper, we examine the special

case of the ‘exponential mean’. This is defined for functions of time  $h(t)$  as

$$\bar{h}(t) = \alpha \int_{-\infty}^t e^{-\alpha(t-s)} h(s) ds, \quad (2.3)$$

where the parameter  $\alpha > 0$  is interpreted as the inverse of an averaging time scale. An advantage of the exponential average is that, in the class of linear averages of the form

$$\bar{h}(t) = \int_{-\infty}^{\infty} k(t-s)h(s) ds \quad (2.4)$$

for some kernel  $k(t-s)$ , it is the only one which leads to a first-order differential equation for the average, namely

$$\frac{d\bar{h}}{dt} = \alpha(h - \bar{h}). \quad (2.5)$$

This makes it possible to compute the average on-the-fly as new values of  $h(t)$  come in. For the computation of Lagrangian means following KV23, the exponential mean avoids the need to treat the averaging time as a (discretised) time variable distinct from the time variable used for the dynamical equations, as is required for the top-hat and other means. The exponential Lagrangian average is simply computed by solving additional PDEs at the same time steps as the dynamical equations. We derive these PDEs next.

### 3. Computing the exponential Lagrangian mean

Particularising (2.1) and (2.2) to the exponential mean (2.3) gives the explicit forms

$$\bar{\varphi}(\mathbf{a}, t) = \alpha \int_{-\infty}^t e^{-\alpha(t-s)} \varphi(\mathbf{a}, s) ds \quad (3.1)$$

$$\text{and} \quad \bar{g}^{\perp}(\bar{\varphi}(\mathbf{a}, t), t) = \alpha \int_{-\infty}^t e^{-\alpha(t-s)} g(\varphi(\mathbf{a}, s), s) ds \quad (3.2)$$

for the mean map and Lagrangian mean of a scalar. (We abuse notation in (3.1) by using the same symbol  $\bar{\varphi}$  for both the mean map and the list of its components  $\bar{\varphi}^i$ . We repeat this abuse with other maps in what follows.) The Lagrangian velocity  $\bar{\mathbf{u}}$  is defined naturally as the time derivative of the mean map:

$$\partial_t \bar{\varphi}(\mathbf{a}, t) = \bar{\mathbf{u}}(\bar{\varphi}(\mathbf{a}, t), t). \quad (3.3)$$

Time differentiation of (3.1) gives

$$\bar{\mathbf{u}}(\mathbf{x}, t) = \alpha(\Xi(\mathbf{x}, t) - \mathbf{x}) \quad (3.4)$$

on substituting  $\mathbf{x} = \bar{\varphi}(\mathbf{a}, t)$ . Here we introduce the so-called lifting map

$$\Xi = \varphi \circ \bar{\varphi}^{-1} \quad (3.5)$$

such that  $\Xi(\mathbf{x}, t)$  is the actual position at time  $t$  of the fluid particle with mean position  $\mathbf{x}$ . We note that  $\bar{\mathbf{u}}$  in (3.4) also results from applying the exponential Lagrangian mean (3.2) to

each component of the velocity field  $\mathbf{u}$ . This follows from the computation

$$\begin{aligned} \alpha \int_{-\infty}^t e^{-\alpha(t-s)} \mathbf{u}(\boldsymbol{\varphi}(\mathbf{a}, s), s) \, ds &= \alpha \int_{-\infty}^t e^{-\alpha(t-s)} \partial_s \boldsymbol{\varphi}(\mathbf{a}, s) \, ds \\ &= \alpha \left[ e^{-\alpha(t-s)} \boldsymbol{\varphi}(\mathbf{a}, s) \right]_{-\infty}^t - \alpha^2 \int_{-\infty}^t e^{-\alpha(t-s)} \boldsymbol{\varphi}(\mathbf{a}, s) \, ds \\ &= \alpha (\boldsymbol{\varphi}(\mathbf{a}, t) - \bar{\boldsymbol{\varphi}}(\mathbf{a}, t)) \\ &= \alpha (\Xi(\mathbf{x}, t) - \mathbf{x}) = \bar{\mathbf{u}}(\mathbf{x}, t), \end{aligned} \quad (3.6)$$

where  $\mathbf{x} = \bar{\boldsymbol{\varphi}}(\mathbf{a}, t)$  and the last equality uses (3.4). We nonetheless refrain from identifying  $\bar{\mathbf{u}}$  with  $\bar{\mathbf{u}}^L$  for reasons that become clear in §5.

The lifting map  $\Xi$  is required for computation of Lagrangian averages. It can be computed by solving the PDE obtained by differentiating the identity

$$\Xi(\bar{\boldsymbol{\varphi}}(\mathbf{a}, t), t) = \boldsymbol{\varphi}(\mathbf{a}, t) \quad (3.7)$$

with respect to  $t$  and substituting  $\mathbf{x} = \bar{\boldsymbol{\varphi}}(\mathbf{a}, t)$  to find

$$\partial_t \Xi + \bar{\mathbf{u}} \cdot \nabla \Xi = \mathbf{u} \circ \Xi. \quad (3.8)$$

Taking (3.4) into account, this is a closed PDE for  $\Xi$  that can be solved alongside the dynamical equations.

Time differentiation of (3.2) gives a PDE for the Lagrangian mean of the scalar field  $g(\mathbf{x}, t)$ , namely

$$\partial_t \bar{g}^L + \bar{\mathbf{u}} \cdot \nabla \bar{g}^L = \alpha (g \circ \Xi - \bar{g}^L). \quad (3.9)$$

We solve this together with (3.8) since  $\Xi$  is required both for  $\bar{\mathbf{u}}$  on the left-hand side and for the composition on the right-hand side. As initial conditions we use  $\Xi(\mathbf{x}, 0) = \mathbf{x}$  and  $\bar{g}^L(\mathbf{x}, 0) = 0$ . This leads to  $\bar{g}^L(\mathbf{x}, t)$ , at least for  $t$  large enough that the integration limit  $t \rightarrow -\infty$  in (3.2) can be replaced by  $t = 0$ .

Eqs. (3.4), (3.8) and (3.9) are key results of this paper. They provide a route for an efficient, easy-to-implement computation of Lagrangian averages leveraging the unique properties of the exponential mean. Eq. (3.9) in particular can be thought of as a Lagrangian version of the ODE (2.5) for the exponential mean.

## 4. Shallow-water example

### 4.1. Implementation

We compute Lagrangian means in a simulation of a turbulent flow interacting with a Poincaré wave in a rotating shallow-water model (e.g. Vallis 2017; Zeitlin 2018). We use the non-dimensional equations for rotating shallow water with characteristic length  $L$ , characteristic velocity  $U$  and characteristic time  $T = L/U$ , that is,

$$\partial_t \mathbf{u} + \mathbf{u} \cdot \nabla \mathbf{u} + Ro^{-1} \hat{\mathbf{z}} \times \mathbf{u} = -Fr^{-2} \nabla h, \quad (4.1a)$$

$$\partial_t h + \nabla \cdot (h\mathbf{u}) = 0, \quad (4.1b)$$

which introduces the Rossby and Froude numbers

$$Ro = \frac{U}{fL} \quad \text{and} \quad Fr = \frac{U}{\sqrt{gH}}. \quad (4.2)$$

Here  $g$  is the gravitational acceleration,  $f$  the Coriolis parameter,  $H$  the mean depth and  $\hat{\mathbf{z}}$  the vertical unit vector.

We solve the dynamical equations (4.1) together with the Lagrangian mean equations (3.8) and (3.9) using a pseudospectral discretisation. To solve exclusively for doubly periodic fields, we express the lifting map  $\Xi$  in terms of the (doubly periodic) displacement map  $\xi(\mathbf{x}, t) = \Xi(\mathbf{x}, t) - \mathbf{x}$  replacing (3.8) by

$$\partial_t \xi + \bar{\mathbf{u}} \cdot \nabla \xi = \mathbf{u} \circ (\text{id} + \xi) - \bar{\mathbf{u}}, \quad (4.3)$$

where  $\text{id}$  denotes the identity map and  $\xi(\mathbf{x}, 0) = 0$ , and (3.9) by

$$\partial_t \bar{g}^L + \bar{\mathbf{u}} \cdot \nabla \bar{g}^L = \alpha(g \circ (\text{id} + \xi) - \bar{g}^L). \quad (4.4)$$

The Lagrangian mean velocity is deduced from  $\xi$  as  $\bar{\mathbf{u}} = \alpha \xi$  obtained from (3.4).

We use of modified version of the code developed by KV23. We discretise (4.1), (4.3) and (4.4) using  $256^2$  grid points/Fourier modes, use an RK4 integrator with time step  $\Delta t = 0.005$  and integrate over the time range  $0 \leq t \leq T = 50$ . For numerical stability, we employ 2/3 dealiasing and add hyperviscous dissipation to the momentum shallow-water equation (4.1a) which amounts to multiplying the Fourier variables  $\hat{\mathbf{u}}(\mathbf{k}, t)$  by  $\exp(-\kappa |\mathbf{k}|^8 \Delta t)$  at each time step. We take  $\kappa = 2.6 \times 10^{-14}$ . We achieve a stable numerical solution of the Lagrangian mean equations (4.3) and (4.4) without any dissipation. However, a form of dissipation may be required to ensure numerical instability in other flow configurations. We use bilinear interpolation to evaluate  $\mathbf{u}$  and  $g$  at the position  $\mathbf{x} + \xi(\mathbf{x}, t)$  as required for (4.3) and (4.4).

We initialise the model with the same initial condition as in KV23 superimposing a geostrophic turbulent flow, obtained by prior solution of a quasi-geostrophic model, and a right travelling mode-1 Poincaré wave. We take the root-mean square velocity of the geostrophic flow as characteristic velocity  $U$  and the length scale of the first Fourier mode as characteristic length  $L$  so that the doubly periodic domain is  $[0, 2\pi]^2$ . The Rossby and Froude number of the geostrophic flow are  $Ro = 0.1$  and  $Fr = 0.5$ . With these parameters, the frequency  $\omega = (Ro^{-2} + Fr^{-2})^{1/2}$  of the mode-1 Poincaré wave is  $\omega = 10.2$  corresponding to a period of 0.62 time units. The wave field in the absence of flow are given by

$$u' = a \cos(x - \omega t), \quad v' = \frac{a}{\omega Ro} \sin(x - \omega t), \quad h' = \frac{a}{\omega} \cos(x - \omega t). \quad (4.5)$$

At the initial time  $t = 0$ , we add these to the geostrophic flow field. We take the amplitude  $a = -1$  so that the maximum wave velocity is as large as the geostrophic flow root-mean-square velocity.

## 4.2. Results

We first consider the Lagrangian mean of the relative vorticity  $\zeta = \partial_x v - \partial_y u$  and thus set  $g = \zeta$  in (4.4). The top row of figure 1 shows  $\zeta$  at  $t = 12.5, 25, 37.5$  and  $50$ . The mode-1 wave which we aim to filter out is a dominant feature. It is distorted by the flow consisting of vortices and filaments familiar in two-dimensional (quasi-geostrophic) turbulence. The middle and bottom rows compare the Lagrangian and Eulerian means  $\bar{\zeta}^L$  and  $\bar{\zeta}$  computed at  $t = 50$  with an inverse averaging time scale  $\alpha = 0.5$ . Both means filter out the wave satisfactorily, but the Eulerian mean blurs the small-scale vorticity structures of the flow as a result of the rapid advection by the velocity field associated with the wave. The Lagrangian mean eliminates this advection by construction.

A qualitatively similar Lagrangian mean field is obtained using the top-hat mean of KV23. However, the exponential mean provides a much simpler way of computing a Lagrangian mean over an entire time interval rather than a single snapshot. In particular, since the exponential Lagrangian mean computation shares the same (small) time step as the solution of the dynamical equations, it resolves the fast wave time scales in the system, making it straightforward to examine the wave signal that remains after averaging.

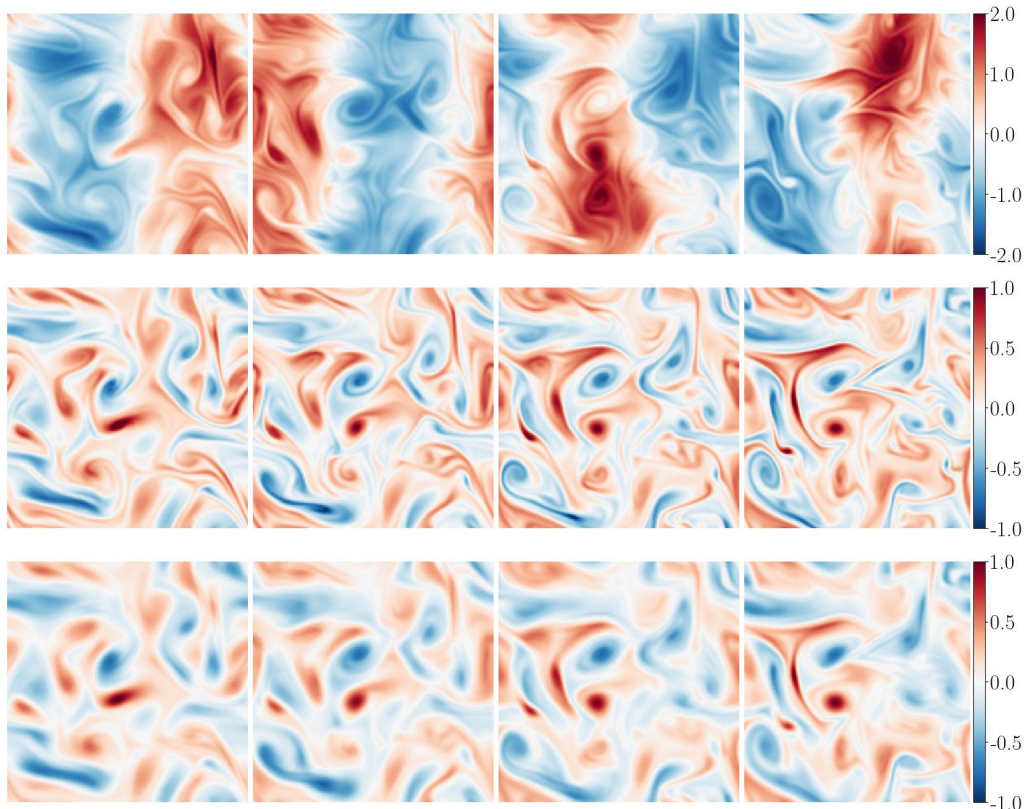


Figure 1: Vorticity field in the rotating shallow-water simulation at  $t = 12.5, 25, 37.5$  and  $50$ : instantaneous vorticity  $\zeta$  (top row), Lagrangian mean vorticity  $\bar{\zeta}^L$  (middle row) and Eulerian mean vorticity  $\bar{\zeta}$  (bottom row). The exponential mean with inverse averaging time scale  $\alpha = 0.5$  is used for the mean vorticity fields in the middle and bottom rows. See also the animation [movie 1](#).

We illustrate this with figure 2, which shows a Hovmöller diagram of  $\zeta$  and  $\bar{\zeta}^L$  at fixed  $x = 0.24$ , and with an animation of the evolution of  $\zeta$ ,  $\bar{\zeta}^L$  and  $\bar{\zeta}$  ([movie 1](#)). The wave signal in the instantaneous field  $\zeta$  is strongly reduced by the exponential averaging, yielding a mean field  $\bar{\zeta}^L$  that captures the slow dynamics well, but the wave signal is not eliminated completely. This is not surprising: the exponential mean is a low-pass filter with a broad frequency response which reduces rather than eliminates high frequencies (its Fourier-domain transfer function at frequency  $\Omega$  is  $(\alpha - i\Omega)^{-1}$ ). This limitation of the exponential mean is also evident in the relation  $\bar{\mathbf{u}} = \alpha \boldsymbol{\xi}$  between the (slow) mean velocity  $\bar{\mathbf{u}}$  and the (fast) displacement  $\boldsymbol{\xi}$ . The notional slowness of  $\bar{\mathbf{u}}$  stems only from the property  $|\bar{\mathbf{u}}| \ll |\partial_t \boldsymbol{\xi}|$ , which is obeyed provided that  $\alpha/\omega \ll 1$ , whereas one can ask for stricter slowness conditions, not satisfied by the exponential mean, which demand that  $|\partial_t^n \bar{\mathbf{u}}| \sim (\alpha/\omega)^n |\partial_t^{n+1} \boldsymbol{\xi}|$  for  $n = 0, 1, 2, \dots$ .

The choice of  $\alpha$  determines which range of frequencies are filtered out effectively by the exponential mean. Figure 3 illustrates the effect of varying  $\alpha$  by showing  $\zeta$  and  $\bar{\zeta}^L$  at the fixed position  $(x, y) = (1.2, 1.2)$  as a function of time for three values of  $\alpha$ , all for which such that  $\alpha/\omega \ll 1$ . Clearly, decreasing  $\alpha$  reduces the magnitude of the fast oscillations induced by the wave. For the smallest value of  $\alpha$ ,  $\alpha = 0.2$ ,  $\bar{\zeta}^L$  differs markedly from the



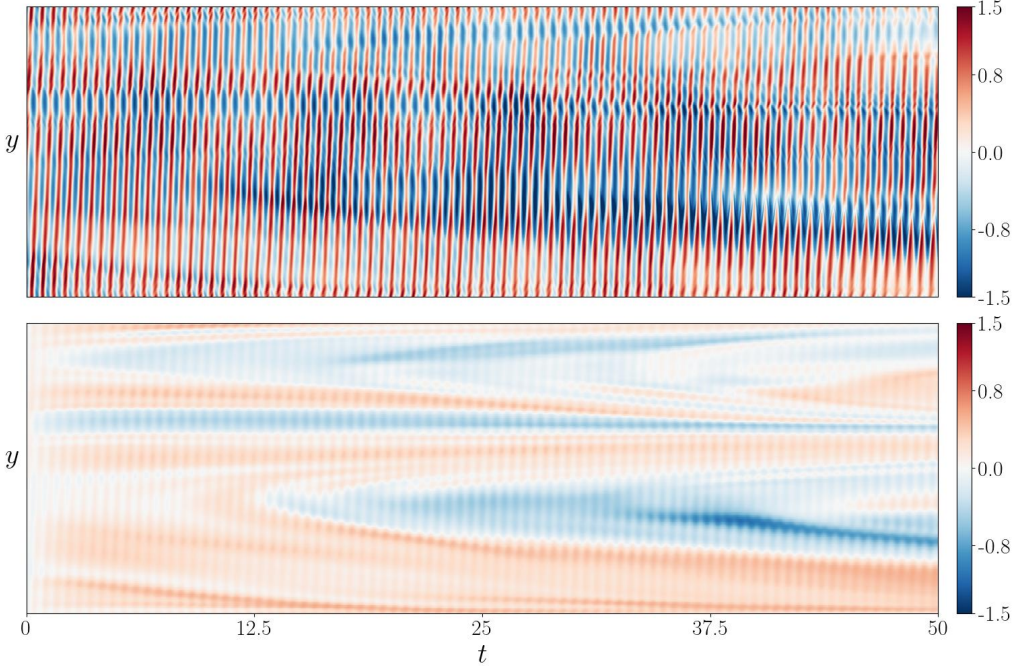


Figure 2: Vorticity  $\zeta$  (top) and its exponential Lagrangian mean  $\bar{\zeta}^L$  with  $\alpha = 0.5$  (bottom) as functions of  $t$  and  $y$  for  $x = 0.24$  in the simulation in figure 1.

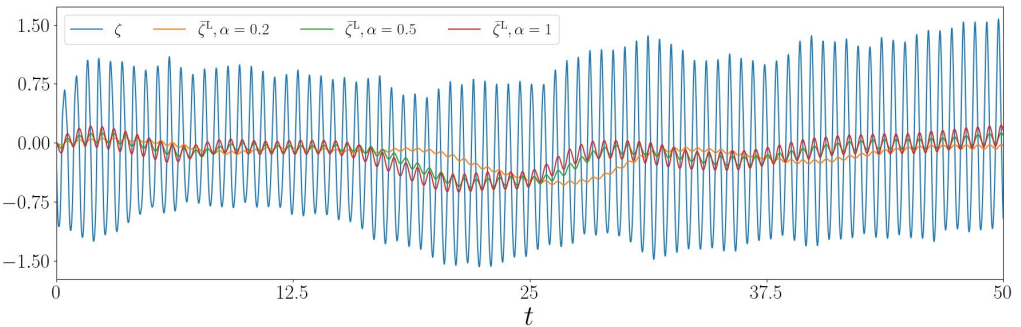


Figure 3: Vorticity at  $(x, y) = (1.2, 1.2)$  as a function of  $t$ : the instantaneous value  $\zeta$  is compared with the exponential Lagrangian average with  $\alpha = 0.2, 0.5$  and  $1$ .

(Eulerian) average that is estimated by eye from the instantaneous  $\zeta$ ; this is a reminder that Lagrangian averaging is non-local in space and depends on the field at positions other than where it is evaluated. In applications, the choice of  $\alpha$  should be guided by the use made of the Lagrangian averaging. In particular, when the aim is to assess the impact of waves on the mean flow, there is a trade off between the requirement to filter out fast waves and the need to retain the dynamically significant time scales of the flow. We return to such applications in §5. Our experimentations show that, for the flow considered,  $\alpha = 0.5$  is a good compromise. This suggests that, more generally, exponential averaging with inverse averaging time  $\alpha$  is effective in filtering out waves of frequencies  $\omega \gtrsim 20\alpha$ .

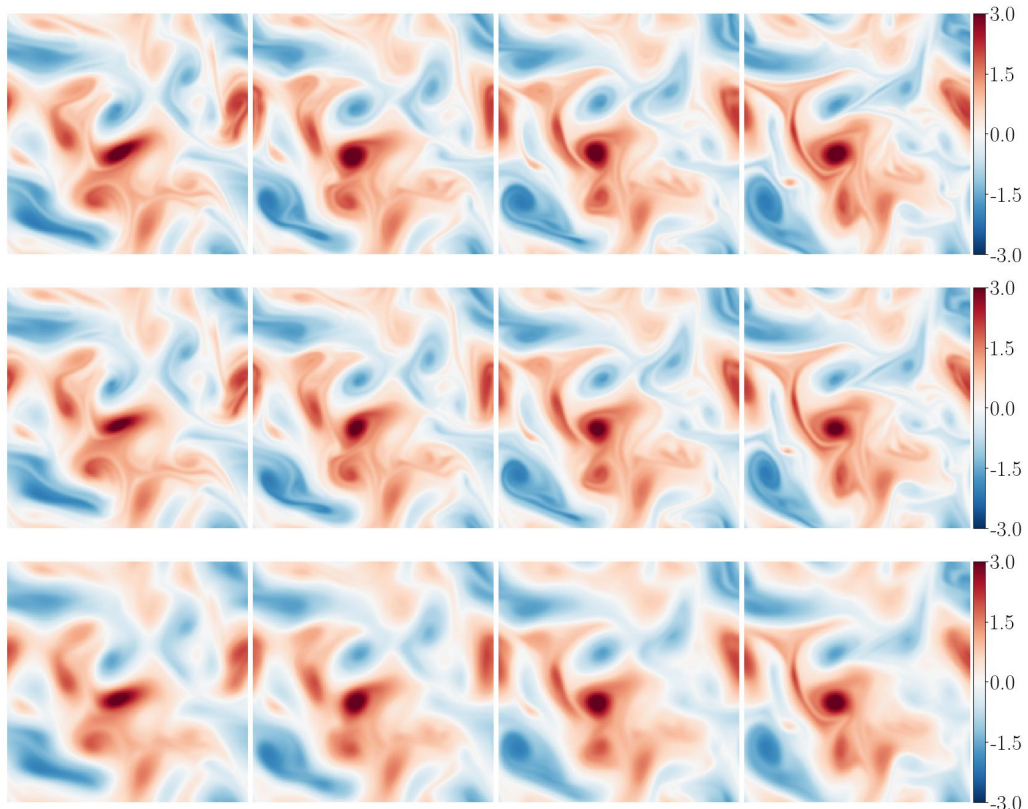


Figure 4: Same as figure 1 but for the potential vorticity anomaly  $q$  at  $t = 12.5, 25, 37.5$  and  $50$ :  $q$  (top row),  $\bar{q}^L$  (middle row) and  $\bar{q}$  (bottom row). See also the animation [movie 2](#).

A scalar of particular interest is the potential vorticity (PV)

$$q = \frac{Ro^{-1} + \zeta}{h} - Ro^{-1} \quad (4.6)$$

which we give here in non-dimensional form with the constant background PV subtracted. Because the PV of the Poincaré wave is zero (at a linear level), it is impacted by the wave in a very different way to the relative vorticity  $\zeta$ : advection by the velocity field associated with the wave induces a fast oscillation of PV structures that are otherwise unaffected. These oscillations limit the usefulness of the Eulerian mean PV compared with the Lagrangian mean PV. We illustrate this in figure 4 which shows snapshots of the PV and of its exponential Lagrangian and Eulerian means. Animations of  $q$ ,  $\bar{q}^L$  and  $\bar{q}$  are available in [movie 2](#). The Eulerian mean PV is blurred whereas the Lagrangian mean retains all the features of the instantaneous field. In the absence of dissipation, the material conservation of  $q$  implies that  $q = q_0 \circ \varphi^{-1}$ , with  $q_0$  the initial PV field, hence  $\bar{q}^L = \overline{q \circ \Xi}$  is the average of  $q_0 \circ \bar{\varphi}^{-1}$  and approximately equal to  $q_0 \circ \bar{\varphi}^{-1}$  itself insofar as  $\bar{\varphi}^{-1}$  can be regarded as slow. Therefore, the Lagrangian mean PV is approximately a rearrangement of the instantaneous PV, thus sharing the same extrema and topology.



## 5. Exponential mean of tensors

A key benefit of Lagrangian averaging is that, when applied to the dynamical equations, it leads to particularly simple mean equations that inherit much of the structure of the original equations and hence preserve properties of inviscid fluids such as the material transport of vorticity and the conservation of Kelvin's circulation (Andrews & McIntyre 1978; Holm 2019, 2002*a,b*; Gilbert & Vanneste 2018). Taking advantage of this requires extending the concept of Lagrangian averaging from the scalar fields considered in §3 to arbitrary tensor fields. We now discuss this extension. We build on the geometric interpretation of GLM in Gilbert & Vanneste (2018) and Gilbert & Vanneste (2024) and refer the reader to these papers for an introduction to the underlying concepts and notation.

### 5.1. Averaging tensors

The extension of the exponential Lagrangian mean to a tensor field  $\tau(\mathbf{x}, t)$  reads

$$(\bar{\varphi}^* \bar{\tau}^L)(\mathbf{a}, t) = \alpha \int_{-\infty}^t e^{-\alpha(t-s)} (\varphi^* \tau)(\mathbf{a}, s) ds. \quad (5.1)$$

Here,  $\bar{\varphi}^*$  and  $\varphi^*$  denotes the pull-backs of the tensor  $\tau$  by  $\bar{\varphi}$  and  $\varphi$  (e.g. Frankel 2004). These take different forms depending on the nature of  $\tau$ : in particular, for scalar fields,

$$(\varphi^* g)(\mathbf{a}, t) = g(\varphi(\mathbf{a}, t), t), \quad (5.2)$$

making (5.1) consistent with (3.2), for (contravariant) vector fields  $\mathbf{v} = v^i(\mathbf{x}, t)\mathbf{e}_i$ ,

$$(\varphi^* \mathbf{v})^i(\mathbf{a}, t) = K^i_j(\mathbf{a}, t) v^j(\varphi(\mathbf{a}, t), t), \quad (5.3)$$

and for 1-forms fields (i.e. covariant vectors or covectors)  $\beta = \beta_i(\mathbf{x}, t) dx^i$ ,

$$(\varphi^* \beta)_i(\mathbf{a}, t) = \beta_j(\varphi(\mathbf{a}, t), t) J^j_i(\mathbf{a}, t). \quad (5.4)$$

The matrix  $J$  in (5.4) is the Jacobian matrix

$$J^j_i(\mathbf{a}, t) = \frac{\partial \varphi^j(\mathbf{a}, t)}{\partial a^i}, \quad (5.5)$$

and  $K$  in (5.3) is its inverse,  $K = J^{-1}$ , i.e. it satisfies  $K^i_k J^k_j = \delta^i_j$ . Note that, when applied to the velocity vector field  $\mathbf{u}$ , (5.1) and (5.3) give a definition of  $\bar{\mathbf{u}}^L$  that differs from the expression (3.6) for  $\bar{\mathbf{u}}$ . The latter expression corresponds to averaging the components of  $\mathbf{u}$  as scalar fields rather than averaging  $\mathbf{u}$  as a vector field. The distinction justifies the notation  $\bar{\mathbf{u}}$  for the mean velocity.

Taking the time derivative of (5.1), applying the push-forward  $\bar{\varphi}_*$  (the inverse of the pull-back) and noting that (3.5) implies that  $\bar{\varphi}_* \varphi^* = \Xi^*$  leads to

$$(\partial_t + \mathcal{L}_{\bar{\mathbf{u}}}) \bar{\tau}^L = \alpha (\Xi^* \tau - \bar{\tau}^L). \quad (5.6)$$

This is the desired extension of (3.9) from scalar fields to arbitrary tensor fields. Here we have introduced the Lie derivative  $\mathcal{L}_{\bar{\mathbf{u}}}$  whose expression differs depending on the nature of the tensor field it applies to. In particular,

$$\mathcal{L}_{\bar{\mathbf{u}}} g = \bar{u}^j \partial_j g, \quad (\mathcal{L}_{\bar{\mathbf{u}}} \mathbf{v})^i = \bar{u}^j \partial_j v^i - v^j \partial_j \bar{u}^i \quad \text{and} \quad (\mathcal{L}_{\bar{\mathbf{u}}} \beta)_i = \bar{u}^j \partial_j \beta_i + \beta_j \partial_i \bar{u}^j \quad (5.7)$$

for scalar, vector and 1-form fields. Eq. (5.6) should be solved together with (3.8) for  $\Xi$  and using (3.4) for  $\bar{\mathbf{u}}$ . For tensor fields other than scalars, the solution requires the evaluation of the derivatives of  $\Xi$  and  $\bar{\mathbf{u}}$  that appear in the pull-back and Lie derivative.

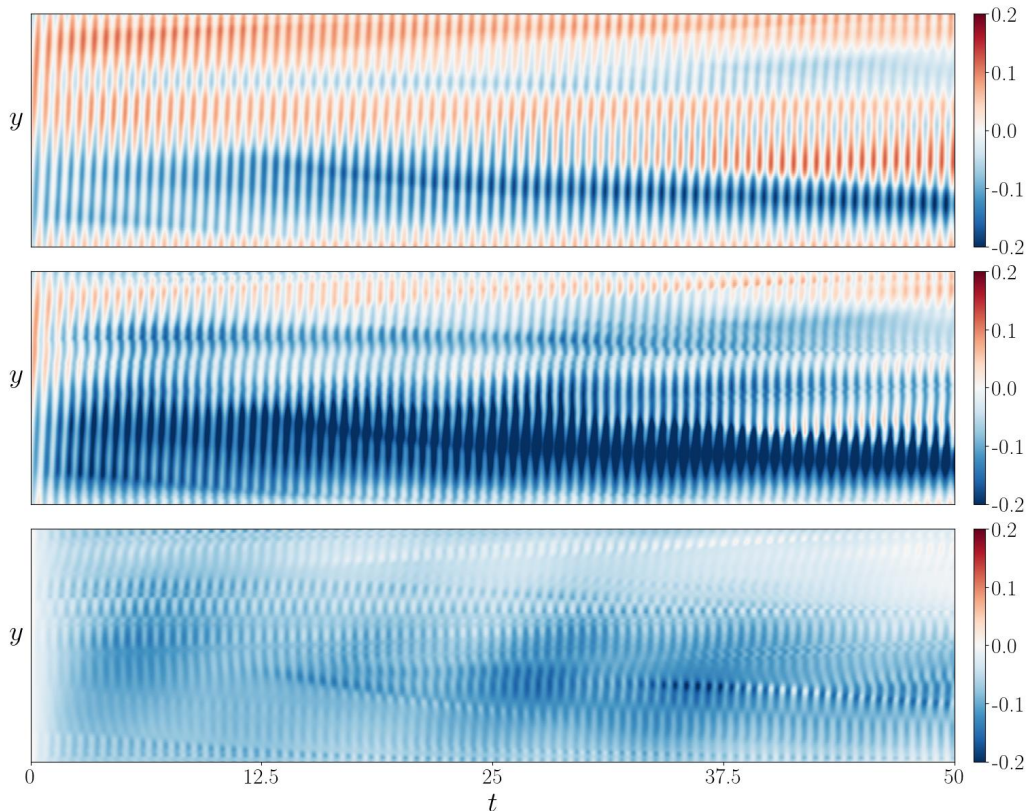


Figure 5: Mean velocity  $\bar{u}_1$  (top), Lagrangian mean momentum  $\bar{v}_1^L$  (middle) and pseudomomentum  $\mathbf{p}_1 = \bar{u}_1 - \bar{v}_1^L$  (bottom) as functions of  $t$  and  $y$  for  $x = 0.24$  in the simulation in figure 1.

## 5.2. Momentum, pseudomomentum and mass

A tensor field of particular interest is the momentum 1-form

$$\boldsymbol{\nu} = \mathbf{u} \cdot d\mathbf{x}. \quad (5.8)$$

It appears as the integrand in Kelvin's circulation and is the central dynamical variable in formulations of the fluid equations best suited for Lagrangian averaging. In Euclidean geometry and Cartesian coordinates, the components of  $\boldsymbol{\nu}$  are identical to those of  $\mathbf{u}$ ,  $\nu_i = u^i$ , but the 1-form nature of  $\boldsymbol{\nu}$  matters for the explicit form of (5.6). This is given by

$$\partial_t \bar{v}_i^L + \bar{u}^j \partial_j \bar{v}_i^L + \bar{v}_j^L \partial_i \bar{u}^j = \alpha \left( \partial_i \Xi^j (\nu_j \circ \Xi) - \bar{v}_i^L \right), \quad (5.9)$$

on using (5.4) and (5.7).

As a proof of concept, we compute the Lagrangian mean momentum  $\bar{\boldsymbol{\nu}}^L$  in the shallow-water simulation of §4. We solve (5.9) and show in figure 5 a comparison between the mean velocity  $\bar{\mathbf{u}}$  and Lagrangian mean momentum  $\bar{\boldsymbol{\nu}}^L$  in the form of Hovmöller diagrams for their first components  $\bar{u}_1$  and  $\bar{v}_1^L$ . According to GLM theory, and ignoring the effect of the Coriolis force for simplicity, the primary impact of perturbations filtered out by the Lagrangian mean on the dynamics of the mean flow is encoded in the difference between  $\bar{\boldsymbol{\nu}}^L$  and  $\bar{\mathbf{u}}$ , or more

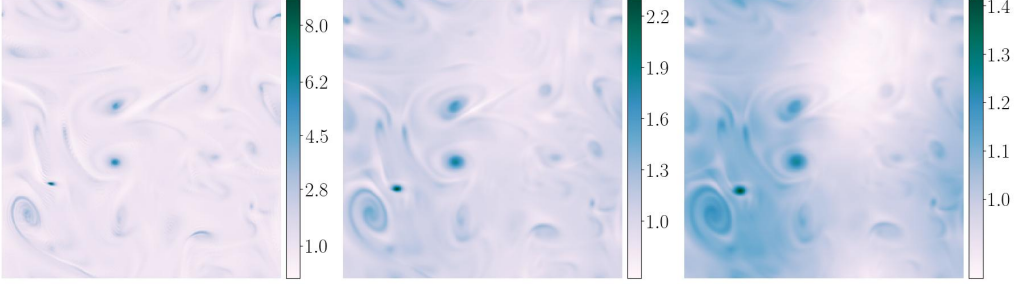


Figure 6: Jacobian  $|\partial_i \Xi^j|$  at  $t = 50$  in the simulation of figure 1 for inverse averaging time  $\alpha = 0.2$  (left), 0.5 (middle) and 1 (right).

precisely in the pseudomomentum, defined in Cartesian coordinates by

$$-\mathbf{p} = \bar{\mathbf{v}}^L - \bar{u}_1 dx_1 - \bar{u}_2 dx_2. \quad (5.10)$$

The bottom panel of figure 5 shows its first component  $p_1$ . The magnitude of  $p_1$  is significantly smaller than that of both  $\bar{u}_1$  and  $\bar{v}_1^L$ , and the same applies to the second components (not shown). This suggests that the Poincaré wave has only a moderate impact on the evolution of the Lagrangian mean flow. The pseudomomentum displays a wave signal – the result of the limitations of the exponential mean discussed in §4.2 – but also low frequency patterns. These capture the impact of the wave on the mean flow and would be the target for parameterisation in closed models describing solely the slow dynamics of the mean flow.

Another tensor of interest is the mass, thought of as the 2-form  $h dx_1 \wedge dx_2$ . Writing

$$\overline{h dx_1 \wedge dx_2}^L = \tilde{h} dx_1 \wedge dx_2, \quad (5.11)$$

which defines the effective height  $\tilde{h}$  (Bühler & McIntyre 1998), we apply (5.6) to find

$$\partial_t \tilde{h} + \nabla \cdot (\tilde{h} \bar{\mathbf{u}}) = \alpha (|\partial_i \Xi^j| (h \circ \Xi) - \tilde{h}), \quad (5.12)$$

where  $|\partial_i \Xi^j| = \partial_1 \Xi^1 \partial_2 \Xi^2 - \partial_2 \Xi^1 \partial_1 \Xi^2$  is the Jacobian of the map  $\Xi$ , and we use that  $\mathcal{L}_{\bar{\mathbf{u}}}(dx_1 \wedge dx_2) = (\nabla \cdot \bar{\mathbf{u}}) dx_1 \wedge dx_2$  and  $\Xi^*(dx_1 \wedge dx_2) = |\partial_i \Xi^j| dx_1 \wedge dx_2$ . The conservation of the Lagrangian mean mass,  $(\partial_t + \mathcal{L}_{\bar{\mathbf{u}}}) \overline{h dx_1 \wedge dx_2}^L = 0$ , implies that the left-hand side of (5.12) vanishes, leaving

$$\tilde{h} = (h \circ \Xi) |\partial_i \Xi^j|. \quad (5.13)$$

(This also follows from the fact that  $\Xi^*(h dx_1 \wedge dx_2) = \bar{\varphi}_*(h_0 dx_1 \wedge dx_2)$  with  $h_0$  the initial height field (cf. Andrews & McIntyre 1978; Bühler 2014).) This shows that the effective height, which controls the mass distribution of the Lagrangian mean flow is not a simple rearrangement of the actual height but depends on the Jacobian  $|\partial_i \Xi^j|$ . This Jacobian is sensitive to the choice of  $\alpha$  and becomes large for small  $\alpha$  because  $\Xi$  then captures part of the slow motion which is exponentially stretching, unlike the wave part.

We illustrate this in figure 6 which shows the Jacobian  $|\partial_i \Xi^j|$  at the end of the shallow-water simulation for  $\alpha = 0.2, 0.5$  and 1. The variations of the Jacobian away from the area-preserving value of 1 increase as  $\alpha$  decreases, corresponding to longer averaging times. For the smallest value  $\alpha = 0.2$ , the averaging time is so long as to overlap with the dynamical time scales of the slow flow; as a result, the map  $\Xi$  differs significantly from the identity. The associated divergence effect, that is, the compressibility of the mean flow arising from the GLM component-wise definition of the mean (Andrews & McIntyre 1978; McIntyre 1988), leads to a Jacobian that does not remain close to 1. This has implications both for

the interpretation of the mean as faithfully representing the dynamics and for numerical computations. In comparison, the largest value  $\alpha = 1$  leads to a Jacobian that remains close to 1, but it does not give a sufficiently long averaging time to filter out the wave effectively.

## 6. Discussion

In this paper, we propose and test a method for the numerical computation of temporal Lagrangian means from simulation data. We adapt the PDE-based algorithm of KV23 to a specific choice of time averaging, namely the exponential mean (2.3). This mean has the unique advantage that all the fields required in the computation satisfy evolution equations with the same time variable as that of the dynamical equations. The equations for the Lagrangian mean fields can therefore be solved on-the-fly, together with the dynamical equations, with no overheads beyond those that result from a few additional equations (for a scalar field  $g$  and in  $n$  dimensions, there are  $n + 1$  additional equations for  $\bar{g}^\perp$  and  $\Xi$ ). This is in contrast with other means such as the top-hat mean used by KV23 and the more sophisticated frequency filters used by Baker *et al.* (2024) which require the solution of a separate initial value problem for each of the times at which the mean fields are desired. A downside of the exponential mean is however its broad frequency response which leads to a reduction rather than elimination of high frequencies from the mean fields. The frequency filters of Baker *et al.* (2024) perform markedly better in this respect.

The availability of a simple and efficient method for the computation of Lagrangian mean fields paves the way for the analysis of realistic simulations of geophysical fluid flows. In particular, it makes it possible to diagnose the effects that waves, or more broadly the fast components of the flow filtered out by averaging, have on the mean flow. According to GLM theory, these are encoded in the pseudomomentum, best thought of as a 1-form (or co-vector) and defined as minus the difference between Lagrangian mean momentum and Lagrangian mean velocity. With this in mind, we consider the exponential averaging of arbitrary tensor quantities and apply the resulting method to the momentum 1-form and to the mass 2-form.

The computations in this paper rely on the standard GLM definition of the mean flow map as a component-wise mean. While this has the advantage of simplicity, it also has drawbacks, primarily the divergence effect associated with the compressibility of the mean flow even for incompressible fluids. In the case of the (compressible) shallow-water model we use here, it leads to changes in the effective height  $\tilde{h}$  that are much larger than changes in the actual height  $h$ . Alternative, more geometric definitions of the mean flow have been proposed that guarantee the incompressibility of the mean velocity for incompressible fluids and, in the shallow-water context, would lead to changes in  $\tilde{h}$  commensurate with those in  $h$  (Soward & Roberts 2010; Gilbert & Vanneste 2018). It would be desirable to develop numerical procedures for the computation of the Lagrangian mean quantities corresponding to these definitions.

**Supplementary data.** Supplementary movies are available as [movie 1](#) and [movie 2](#).

**Acknowledgements.** We are grateful to O. Bühler for suggesting the use of the exponential mean for Lagrangian averaging.

**Funding.** L.E.B. and H.A.K. are supported by the UK Engineering and Physical Sciences Research Council grants EP/X028135/1 and grant EP/Y021479/1, respectively. J.V. is supported by the UK Natural Environment Research Council grant NE/W002876/1.

**Declaration of Interests.** The authors report no conflict of interest.

**Author ORCIDs.** A. Minz, <https://orcid.org/0009-0003-4209-3428>; L.E. Baker, <https://orcid.org/0000-0003-2678-3691>; H. A. Kafiabad, <https://orcid.org/0000-0002-8791-9217>; J. Vanneste, <https://orcid.org/0000-0002-0319-589X>

## REFERENCES

- ANDREWS, D. G. & MCINTYRE, M. E. 1978 An exact theory of nonlinear waves on a Lagrangian-mean flow. *Journal of fluid Mechanics* **89** (4), 609–646.
- BACHMAN, S. D., SHAKESPEARE, C. J., KLEYPAS, J., CASTRUCCIO, F. S. & CURCHITSER, E. 2020 Particle-based Lagrangian filtering for locating wave-generated thermal refugia for coral reefs. *Journal of Geophysical Research: Oceans* **125** (7), e2020JC016106.
- BAKER, L. E., KAFIABAD, H. A. & VANNESTE, J. 2024 Lagrangian filtering for wave–mean flow decomposition Preprint, arXiv:2406.03477.
- BÜHLER, O. 2014 *Waves and mean flows*. Cambridge University Press.
- BÜHLER, O. & MCINTYRE, M. E. 1998 On non-dissipative wave–mean interactions in the atmosphere or oceans. *Journal of Fluid Mechanics* **354**, 301–343.
- FRANKEL, T. 2004 *The geometry of physics*, 2nd edn. Cambridge University Press.
- GILBERT, A. D. & VANNESTE, J. 2018 Geometric generalised Lagrangian-mean theories. *Journal of Fluid Mechanics* **839**, 95–134.
- GILBERT, A. D. & VANNESTE, J. 2024 Geometric approaches to Lagrangian averaging. *Annual Review of Fluid Mechanics* In press, arXiv:2405.04394.
- HOLM, D. D. 2002a Lagrangian averages, averaged Lagrangians, and the mean effects of fluctuation in fluid dynamics. *Chaos* **12**, 518–530.
- HOLM, D. D. 2002b Variational principles for Lagrangian-averaged fluid dynamics. *J. Phys. A. Math. Gen.* **35**, 679–668.
- HOLM, D. D. 2019 Stochastic closures for wave–current interaction dynamics. *J. Nonlinear Sci.* **29**, 2987–3031.
- JONES, C. S., XIAO, Q., ABERNATHEY, R. P. & SMITH, K. S. 2023 Using Lagrangian filtering to remove waves from the ocean surface velocity field. *Journal of Advances in Modeling Earth Systems* **15** (4), e2022MS003220.
- KAFIABAD, H. A. 2022 Grid-based calculation of the Lagrangian mean. *Journal of Fluid Mechanics* **940**, A21.
- KAFIABAD, H. A. & VANNESTE, J. 2023 Computing Lagrangian means. *Journal of Fluid Mechanics* **960**, A36.
- MCINTYRE, M. E. 1988 A note on the divergence effect and the Lagrangian-mean surface elevation in periodic water waves. *Journal of Fluid Mechanics* **189**, 235–242.
- NAGAI, T., TANDON, A., KUNZE, E. & MAHADEVAN, A. 2015 Spontaneous generation of near-inertial waves by the Kuroshio front. *Journal of Physical Oceanography* **45** (9), 2381–2406.
- SHAKESPEARE, C. J., GIBSON, A. H., HOGG, A. M., BACHMAN, S. D., KEATING, S. R. & VELZEBOER, N. 2021 A new open source implementation of Lagrangian filtering: A method to identify internal waves in high-resolution simulations. *Journal of Advances in Modeling Earth Systems* **13** (10).
- SHAKESPEARE, C. J. & HOGG, A. M. 2017 Spontaneous surface generation and interior amplification of internal waves in a regional-scale ocean model. *Journal of Physical Oceanography* **47** (4), 811–826.
- SHAKESPEARE, C. J. & HOGG, A. M. 2018 The life cycle of spontaneously generated internal waves. *Journal of Physical Oceanography* **48** (2), 343–359.
- SHAKESPEARE, C. J. & HOGG, A. M. 2019 On the momentum flux of internal tides. *Journal of Physical Oceanography* **49** (4), 993–1013.
- SOWARD, A. M. & ROBERTS, P. H. 2010 The hybrid Euler–Lagrange procedure using an extension of Moffatt’s method **661**, 45–72.
- VALLIS, G. K. 2017 *Atmospheric and oceanic fluid dynamics*. Cambridge University Press.
- ZEITLIN, V. 2018 *Geophysical fluid dynamics: understanding (almost) everything with rotating shallow water models*. Oxford University Press.